Ammonia as hydrogen carrier for transportation ; investigation of the ammonia exhaust gas fuel reforming

Wang, Wentao; Herreros, José M.; Tsolakis, Athanasios; York, Andrew P.e.

DOI:
10.1016/j.ijhydene.2013.05.144

Document Version
Publisher's PDF, also known as Version of record

Citation for published version (Harvard):
Wang, W, Herreros, JM, Tsolakis, A & York, APE 2013, 'Ammonia as hydrogen carrier for transportation ; investigation of the ammonia exhaust gas fuel reforming', *International Journal of Hydrogen Energy*, vol. 38, no. 23, pp. 9907-9917. https://doi.org/10.1016/j.ijhydene.2013.05.144

Available online at www.sciencedirect.com

SciVerse ScienceDirect

journal homepage: www.elsevier.com/locate/he

Ammonia as hydrogen carrier for transportation; investigation of the ammonia exhaust gas fuel reforming☆

Wentao Wang [a], José M. Herreros [a], Athanasios Tsolakis [a,*], Andrew P.E. York [b]

[a] School of Mechanical Engineering, University of Birmingham, Edgbaston B15 2TT, UK
[b] Johnson Matthey Technology Centre, Blount's Court, Sonning Common, Reading RG4 9NH, UK

ARTICLE INFO

Article history:
Received 25 March 2013
Received in revised form
21 May 2013
Accepted 26 May 2013
Available online 24 June 2013

Keywords:
Ammonia
Hydrogen
Reforming
Diesel
Emissions

ABSTRACT

In this paper we show, for the first time, the feasibility of ammonia exhaust gas reforming as a strategy for hydrogen production used in transportation. The application of the reforming process and the impact of the product on diesel combustion and emissions were evaluated. The research was started with an initial study of ammonia autothermal reforming (NH_3 – ATR) that combined selective oxidation of ammonia (into nitrogen and water) and ammonia thermal decomposition over a ruthenium catalyst using air as the oxygen source. The air was later replaced by real diesel engine exhaust gas to provide the oxygen needed for the exothermic reactions to raise the temperature and promote the NH_3 decomposition. The main parameters varied in the reforming experiments are O_2/NH_3 ratios, NH_3 concentration in feed gas and gas – hourly – space – velocity (GHSV). The O_2/NH_3 ratio and NH_3 concentration were the key factors that dominated both the hydrogen production and the reforming process efficiencies: by applying an O_2/NH_3 ratio ranged from 0.04 to 0.175, 2.5–3.2 l/min of gaseous H_2 production was achieved using a fixed NH_3 feed flow of 3 l/min. The reforming reactor products at different concentrations (H_2 and unconverted NH_3) were then added into a diesel engine intake. The addition of considerably small amount of carbon – free reformate, i.e. represented by 5% of primary diesel replacement, reduced quite effectively the engine carbon emissions including CO_2, CO and total hydrocarbons.

1. Introduction

The use of hydrogen in internal combustion engines has long been believed to be beneficial in terms of emissions reduction such as HCs, CO, CO_2 and particulate emissions [1,2]. Additionally, its utilisation has been proven to be effective in enhancing automotive aftertreatment performance especially at low engine exhaust gas temperatures [3,4]. However, its low volumetric energy density and its high transportation cost make on – board hydrogen storage difficult [5]. Previous studies have shown that H_2 can be produced by means of hydrocarbon reforming [6,7]. This method can be also adopted for the purpose of on-board reforming of hydrocarbon fuel i.e., using recovered heat and oxidant from exhaust gases for

* *Corresponding author*. Tel.: +44 (0) 121 414 4170; fax: +44 (0) 121 414 7484.
E-mail address: a.tsolakis@bham.ac.uk (A. Tsolakis).

0360-3199/$ – see front matter
http://dx.doi.org/10.1016/j.ijhydene.2013.05.144

driving fuel reforming. This is considered as a potential solution to deal with the hydrogen storage issue [8]. Recently, increasing numbers of studies have shown that hydrogen production can be implemented through ammonia thermal decomposition for small scale fuel cell power systems [9–12]. Decomposition of ammonia is by definition COx free, and CO_2 yielded during ammonia synthesis can be sequestrated on-site at the production plants [13–15]. Thus using ammonia as a hydrogen source is potentially an alternative to the conventional hydrocarbon reforming and makes the on-board hydrogen production free of COx.

Ammonia has been overlooked in the past for vehicular applications; both as a fuel and a hydrogen carrier. In general, its low heating value on mass basis indicates ammonia has less energy for combustion than conventional fossil fuels i.e. gasoline and diesel. However, the stoichiometric air – fuel ratio for ammonia is much lower compared to diesel fuel. This results in ammonia having an LHV of 2.64 MJ per kg of stoichiometric mixture, which is comparable to that of diesel (2.77 MJ/kg) [16]. Nonetheless, because of ammonia's relatively high auto-ignition temperature (651 °C compared to 254 °C for diesel), complete in-cylinder combustion of ammonia is difficult, which leads to significant emission of NH_3 [17]. It should be noticed that 1 mol of ammonia contains 1.5 mol of hydrogen, which is 17.8% by weight or 108 kg – H_2/m^3 embedded in liquid ammonia at 20 °C. Comparing this to the most advanced hydrogen storage systems, e.g. metal hydrides, which store H_2 up to 25 kg/m^3, the advantage of ammonia in carrying hydrogen per unit volume is significant [18]. Therefore, using hydrogen extracted from ammonia appears to be more beneficial than combusting ammonia directly in an IC engine. Zamfirescu [13] in a recent study compared NH_3 with other common fuels such as gasoline, CNG, LPG and methanol, showing that NH_3 is competitive to these fuels in terms of gravimetric, volumetric and energetic costs (see in Table 1). Based on this study, a further comparison between each fuel's molar hydrogen carrying ability per unit mass, volume and cost can be made, which indicates ammonia is a more affordable hydrogen carrier, Table 2.

In addition to that, the storage, distribution and transportation infrastructure of ammonia is established [19], with 100 million tonnes of ammonia being delivered each year. Thus the existing production and handling system of ammonia reveal a great potential in expanding its usage to vehicle applications as a sustainable fuel [20]. Ammonia has already been applied but in the form of urea on today's heavy duty diesel vehicles for catalytic aftertreatment systems for NOx reduction. Therefore special technology and regulation for safe storage of ammonia on passenger cars should be developed or an additional step of thermo-catalytic conversion of urea to ammonia should be applied as shown in the literature [21].

As reported in earlier studies, a temperature higher than 500 °C is required for catalytic NH_3 decomposition in order to achieve stable NH_3 conversion and high H_2 production [5,22–24]. However, for on-board applications the exhaust gas temperature of a typical diesel engine is only in the range of 150–400 °C. Thus a mechanism is required to raise the temperature of the gas stream for the purpose of on-board NH_3 decomposition. The new approach is to apply the same principle as that of autothermal reforming (ATR) and exhaust gas fuel reforming, where part of the fuel is oxidised to provide the energy needed by a subsequent fuel reforming mechanism to produce H_2. If sufficient ammonia oxidation takes place, the endothermic ammonia decomposition can be self – sustaining using the provided heat.

The expected selective catalytic oxidation of ammonia (into nitrogen and water) and NH_3 decomposition reactions are expressed by Eqs. (1) and (2), respectively. The desired combination is shown by Eq. (3).

$$4NH_3 + 3O_2 = 6H_2O + 2N_2; \quad \Delta H_r = -1260 kJ/mol \tag{1}$$

$$2NH_3 = 3H_2 + N_2; \quad \Delta H_r = +46 kJ/mol \tag{2}$$

$$NH_3 + xO_2 = 2xH_2O + (1.5 - 2x)H_2 + 0.5N_2; \quad x < 0.75 \tag{3}$$

In Eq. (3), x represents the O_2/NH_3 molar ratio, a parameter which controls the intensity of the exothermic portion in the overall process, which can in turn determine the stoichiometric yield of hydrogen. In the current study, air is used to provide the oxygen needed by the reaction and is referred NH_3 – ATR throughout. Furthermore, if diesel engine exhaust is used to provide the O_2, and part of the exhaust heat is recovered as a primary energy source for the reaction then the NH_3 – ATR is transformed into NH_3 exhaust gas reforming.

To summarise, in this research, three different experiments were performed and analysed. Firstly, the catalytic NH_3 decomposition was studied at different temperatures. Secondly, the oxidative mechanism of ammonia and NH_3 decomposition were combined enabling NH_3 – ATR and NH_3 exhaust

Table 1 – Comparison of ammonia with other fuels including hydrogen (adapted from C. Zamfirescu and I. Dincer, Ammonia as a green fuel and hydrogen source for vehicular applications. Fuel Processing Technology, 2009. 90(5): p. 729–737).

Fuel/storage	P [bar]	Density [kg/m^3]	HHV [MJ/kg]	HHV′ [GJ/m^3]	c [CN$/kg]	C [CN$/m^3]	C/HHV′ [CN$/GJ]
Gasoline, C_8H_{18}/liquid	1	736	46.7	34.4	1.36	1000	29.1
CNG, CH_4/integrated storage	250	188	42.5	10.4	1.20	226	28.2
LPG, C_3H_8/pressurised tank	14	388	48.9	19.0	1.41	548	28.8
Methanol, CH_3OH/liquid	1	786	14.3	11.2	0.54	421	37.5
Hydrogen, H_2/metal hydrides	14	25	142.0	3.60	4.00	100	28.2
Ammonia, NH_3/pressurised tank	10	603	22.5	13.6	0.30	181	13.3

HHV: higher heating value per kg, HHV′: higher heating value per m^3, c: cost per kg, C: cost per m^3.

Table 2 – Further comparison of ammonia with other fuels based on the data listed in Table 1.

Fuel/storage	Hydrogen content [kmol/m^3]	Hydrogen content [kmol/kg]	C[1] [CN$/kmol]
Gasoline, C_8H_{18}/liquid	116.2	0.16	8.5
CNG, CH_4/integrated storage	47	0.25	4.8
LPG, C_3H_8/pressurised tank	70.5	0.18	7.8
Methanol, CH_3OH/liquid	98.3	0.13	4.2
Ammonia, NH_3/pressurised tank	106.4	0.18	1.7

C[1]: Cost of per k mol of carried hydrogen regarding the fuel as hydrogen carrier.

gas reforming. Finally, the yielded reformate (H_2 and unconverted NH_3) was sent back to a diesel engine to examine how a reforming system affects the combustion process and emissions.

2. Experimental and methodology

2.1. Catalyst

In this study, a ruthenium catalyst was chosen, given its activity in both ammonia oxidation [25] and decomposition [22,26]. The catalyst was provided by Johnson Matthey and coated on 1/8 inch OD γ-Al_2O_3 pellet supports with a loading ratio of 2% by weight.

2.2. Test setup

All reforming tests were carried out in a laboratory reforming reactor, which is shown in Fig. 1. The catalyst was loaded inside a stainless steel reactor (15 mm in diameter) that was held vertically within a tube furnace. At the centre of the catalyst bed, a tubular sheath was fitted, which was made from a stainless steel tube with one end sealed. In order to investigate the process's thermal behaviour, a k-type thermocouple was inserted into the sheath to record the reaction temperature along the catalyst bed. Ammonia was supplied by a gas bottle and injected into the reactor, controlled by a flow metre. Nitrogen and air were introduced at separate inlets of the reactor. Before each experiment, inert nitrogen was initially introduced through the reactor to make sure the temperature gradient along the catalyst bed was minimised. For ammonia exhaust gas reforming part of the diesel engine exhaust was extracted from the exhaust manifold and was introduced into the reactor. The exhaust flow rate was controlled to meet different O_2/NH_3 ratios. The product gas was analysed downstream of the reactor. Hydrogen was measured using an HP 5890 series II gas chromatograph (GC) with thermal conductivity detector (TCD) sensor and signal integrator, using argon as the carrier gas. O_2 was measured using an AVL DIGAS 440 non-dispersive IR analyser. NH_3 and all other nitrogen contained species (NO, N_2O and NO_2) were recorded by FTIR (Fourier Transform Infrared Spectroscopy), MKS MultiGas 2030. For ammonia exhaust gas reforming, FTIR was also used to record species such as CO, CO_2 and total hydrocarbons emitted from the engine.

2.3. Test procedure

The catalyst's activity in ammonia decomposition was studied first. Test conditions including catalyst inlet temperature, gas-hourly-space-velocity (GHSV) and catalyst inlet NH_3 concentrations were varied (Table 3). Following that NH_3 – ATR was performed at two catalyst loadings: 8 g and 16 g, whereas NH_3 exhaust gas reforming was studied over the 16 g catalyst only. A NH_3 flow of 3 l/min was used throughout the NH_3 – ATR and Exhaust gas reforming. Air and engine exhaust were added into the NH_3 flow at varying O_2/NH_3 ratios and NH_3 concentrations (Table 4). A 400 °C reactor temperature was maintained using a furnace to simulate the diesel exhaust temperature at mid – high load operation to give the reactor the primary heat. Finally, the reformer system was connected in a closed loop configuration (Fig. 1). Reformates with different compositions were recirculated back to the engine intake while the engine was operated at a constant load of 4 bar IMEP and 1500 rpm. Engine performance and emissions with reformate addition were recorded. The engine exhaust composition for the diesel baseline condition (no reformate addition) is summarised in Table 5.

2.4. Reforming process efficiency

The process efficiency η was defined as the lower combustion enthalpy rate (kJ/sec) of the product stream divided by the lower combustion enthalpy rate (kJ/sec) of the reactant stream. Here, the product stream can be either defined as the produced H_2 alone or H_2 combined with any unconverted NH_3 (both can be considered as fuels to the engine). Thus two efficiencies, namely hydrogen efficiency and reforming process efficiency can be adopted to evaluate the reforming performance. These are defined by Eqs. (4) and (5) below:

$$\eta_{H_2}(\%) = \frac{LCV_{H_2} \times \dot{m}_{H_2}}{LCV_{NH_3} \times \dot{m}_{NH_3}} \times 100\% \quad (4)$$

$$\eta_{ref}(\%) = \frac{(LCV_{H_2} \times \dot{m}_{H_2}) + (LCV_{NH_3} \times \dot{m}_{NH_3})}{LCV_{NH_3} \times \dot{m}_{NH_3}} \times 100\% \quad (5)$$

where LCV_{H_2} and LCV_{NH_3} are the lower calorific values of the produced H_2 and the gas feed NH_3, whereas $\dot{m}_{NH_3}$ and $\dot{m}_{H_2}$ are the mass flow rates of NH_3 and H_2 respectively.

3. Results and discussion

3.1. NH_3 decomposition over Ru – Al_2O_3 catalyst

3.1.1. Temperature effect

Fig. 2(a) depicts the decomposition of pure NH_3 at different reactor inlet temperatures. In addition to experimental results, an equilibrium calculation for NH_3 decomposition was made using an STANJAN equilibrium model (v 3.91, Stanford University) at the same temperatures as those of the

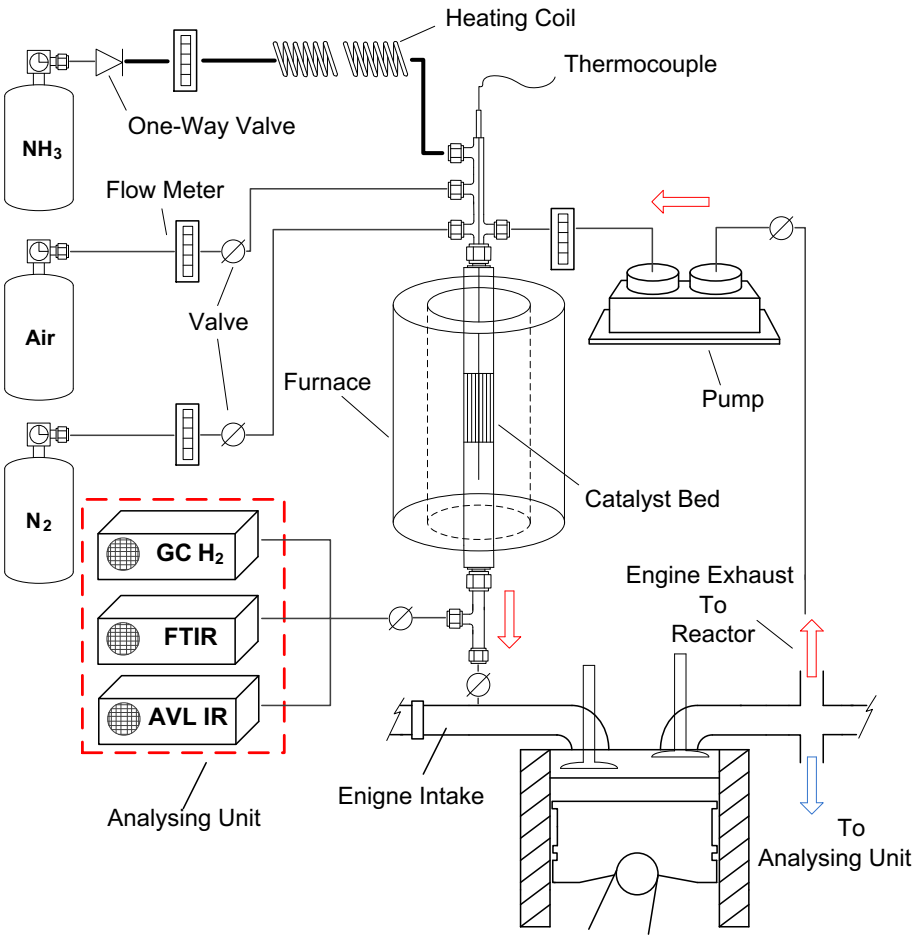

Fig. 1 – Schematic diagram of the test setup.

experimental studies. As predicted by the equilibrium simulation, increased temperature leads to increased NH_3 conversion due to enhanced decomposition kinetics and rate [27]. 100% conversion without catalytic promotion is calculated for temperatures as low as 300 °C. However, when the non-catalytic decomposition was experimentally performed over the plain γ-Al_2O_3 pellet support, no significant NH_3 conversion was observed until the reactor inlet temperature reached 500 °C. The same discrepancy was observed in literature [22] and [28], which implies the equilibrium of non – catalytic NH_3 decomposition was hard to achieve at lower reaction temperatures. Hence, catalytic assistance must be adopted for easier activation: in the presence of ruthenium catalyst, the NH_3 decomposition light off temperature was reduced to 300 °C in the current study, and NH3 conversion was higher, than with only alumina, across the whole temperature range.

From the results presented, it is clear that to achieve NH_3 decomposition in the relatively low temperature range applicable to diesel exhaust i.e. 150–400 °C, the decomposition needs to be accompanied by an exothermic reaction. Therefore, adding an oxygen containing flow (air or exhaust) into the reactor is needed to promote the desired autothermal reaction, i.e. Eq. (3). This results in a variation in GHSV (increased total flow), and in diluted NH_3 feed (NH_3 mixed with oxygen containing flow). Thus prior to the NH_3 – ATR and NH_3 exhaust gas reforming, both GHSV and NH_3 inlet concentration were varied separately to study their impacts on the catalyst activity.

3.1.2. *GHSV effect*

As shown by Fig. 2(b), when the catalyst inlet temperature was fixed at 800 °C, increasing GHSV decreased the ammonia conversion from around 95% at 18000 h^{-1} –75% at 36000 h^{-1}.

Table 3 – Test conditions for NH_3 decomposition.

	NH_3 (l/min)	N_2 (l/min)	Total flow (l/min)	NH_3 (%)	Cat. inlet temp (°C)	GHSV (h^{-1})
Temperature effect	2	–	2	100	300–800	18000
GHSV effect	2–4	–	2–4	100	800	18000–36000
NH_3 Conc. effect	2–4	0–2	4	50–100	300–800	36000

Table 4 – Test conditions for NH_3 – ATR and NH_3 exhaust gas reforming.

O_2/NH_3	8 g catalyst bed (NH_3 – ATR)			16 g catalyst bed (NH_3 – ATR)			16 g catalyst bed (NH_3 Exhst. Ref.)		
	Tot. Flow (l/min) (NH_3 + Air)	GHSV (h^{-1})	NH_3 Conc. (%)	Tot. Flow (l/min) (NH_3 + Air)	GHSV (h^{-1})	NH_3 Conc. (%)	Tot. Flow (l/min) (NH_3 + Exh)	GHSV (h^{-1})	NH_3 Conc. (%)
0.04	–	–	–	3 + 0.67	13392	84	3 + 0.79	14230	79.05
0.06	3 + 0.86	28928	77.78	3 + 0.86	14464	77.78	3 + 1.19	15720	71.56
0.08	3 + 1.14	31071	72.41	3 + 1.14	15535	72.41	3 + 1.58	17210	65.37
0.09	3 + 1.29	32142	70.00	3 + 1.29	16071	70.00	3 + 1.78	17955	62.65
0.12	3 + 1.71	35357	63.64	3 + 1.71	17678	63.64	3 + 2.38	20190	55.72
0.15	3 + 2.14	38571	58.33	3 + 2.14	19285	58.33	3 + 2.98	22425	50.16
0.175	3 + 2.50	41250	54.55	3 + 2.50	20625	54.55	3 + 3.47	24288	46.32

This is due to reduced residence time of the NH_3 over the catalyst at the region where the endothermic reaction is active (i.e. will be described in 3.2 sections) resulting in lowered decomposition efficiencies [29].

3.1.3. *NH_3 concentration effect*

Fig. 2(c) illustrates the ammonia conversion as a function of temperature and ammonia concentration in the feed gas. Instead of using pure NH_3, nitrogen was co-fed into the reactant stream. The total inlet flow was kept constant at 4 l/min, resulting in a GHSV of 36000 h^{-1}. It is shown that as the inlet ammonia concentration reduced, the NH_3 conversion increased for a fixed temperature. In earlier studies, hydrogen was found to be inhibitive to NH_3 decomposition. This is because the NH_3 decomposition is limited by a chemical equilibrium between the forward and reverse reactions. A high H_2 partial pressure and a low reaction temperature will contribute to a retarded forward rate of the NH_3 decomposition [30–34]. This explains the shift of NH_3 conversion to higher temperatures as the ammonia concentration in the feed gas increased. When the NH_3 concentration is higher in a constant reactant flow, the amount of H_2 produced is higher and thus the inhibition is more pronounced [5]. The other product of the reaction, N_2, is seen to have negligible influence on the forward rate [5,30,32]. In the current study, nitrogen behaved mainly as an inert gas, which diluted the inlet NH_3 to lower concentrations. In this case, reactions with lower inlet NH_3 concentrations show similar conversions at lower temperatures as those with high concentrations of NH_3.

3.2. *Combined NH_3 oxidation and decomposition: NH_3 – ATR and NH_3 exhaust gas reforming*

3.2.1. *Temperature profiles*

In Fig. 3 (a) – (c), the thermal behaviour of the combined reaction (Eq. (3)) at different O_2/NH_3 ratios was reflected by the temperature profile along the catalyst bed. For both NH_3 – ATR and NH_3 exhaust gas reforming, the reactor temperature increased abruptly near the catalyst inlet and declined thereafter. The temperature rise at catalyst inlet was due to NH_3 oxidation (Eq. (1)); the decrease was associated with the endothermic ammonia decomposition (Eq. (2)) and the reactor heat losses [8]. Such observation is in agreement with previous researches [35,36], where mechanisms of exothermic and endothermic were combined and performed.

In general, by varying the O_2/NH_3 ratio from 0.04 to 0.175 in both NH_3 – ATR and exhaust gas reforming, the temperature increase along the catalyst bed was enhanced, meaning increased oxygen input promoted the exothermic reaction. In addition to that, the higher the O_2/NH_3 ratio, the larger the temperature drop in the endothermic area, indicating improved NH_3 decomposition along the catalyst bed (this will be confirmed by increased hydrogen formation shown in the next section).

For NH_3 – ATR (Fig. 3(a) and (b)), similar temperature increases were observed over the 8 g and 16 g catalyst beds. However, compared to the 8 g catalyst bed, the temperature decrease was found to be more pronounced at the 16 g catalyst at each tested O_2/NH_3 ratio. This is caused by the greatly increased residence time over the 16 g catalyst strengthening the NH_3 decomposition through a better use of the available enthalpy [29].

When NH_3 – exhaust mixtures were introduced into the 16 g catalyst, the rise in temperature profiles (Fig. 3(c)) were slightly weakened at each O_2/NH_3 condition compared to those for the tests with air. As the engine exhaust contains only 10–15% oxygen by volume, the flow of the exhaust required to maintain the same O_2/NH_3 ratio was increased from that of the air, and so was the GHSV (Table 4). The main diesel exhaust gas components (e.g. CO_2 and H_2O) are known as heat absorbers due to their relatively large specific heat capacities [37]. Therefore, the temperature decrease in the reactor could be associated with the heat absorption of those species.

3.2.2. *NH_3 conversion and H_2 production*

The NH_3 conversion at different O_2/NH_3 ratio is depicted in Fig. 4(a) for NH_3 – ATR over the 8 g and 16 g catalysts. The

Table 5 – Engine exhaust composition at 4 bar IMEP and 1500 rpm.

CO_2 (%)	CO (ppm)	THC (ppm)	NO (ppm)	NO_2 (ppm)	N_2O (ppm)	NOx (ppm)	H_2O (%)	O_2 (%)
5.3	127.5	577	750	40	0	790	5.1	15.1

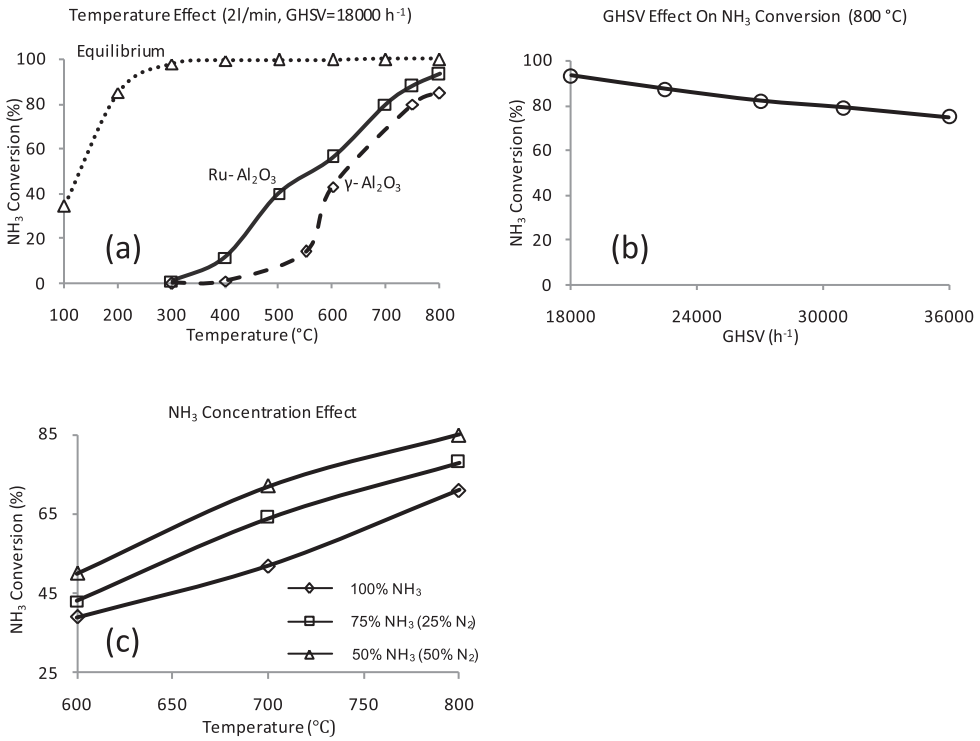

Fig. 2 – NH_3 decomposition over Ru – Al_2O_3 catalyst: (a) 2 l/min (GHSV = 18000 h^{-1}) of pure ammonia decomposed at different temperatures, (b) 2–4 l/min of pure ammonia decomposition at different GHSV, and (c) ammonia conversion at different NH_3 concentrations in the NH_3 – N_2 mixtures and temperatures.

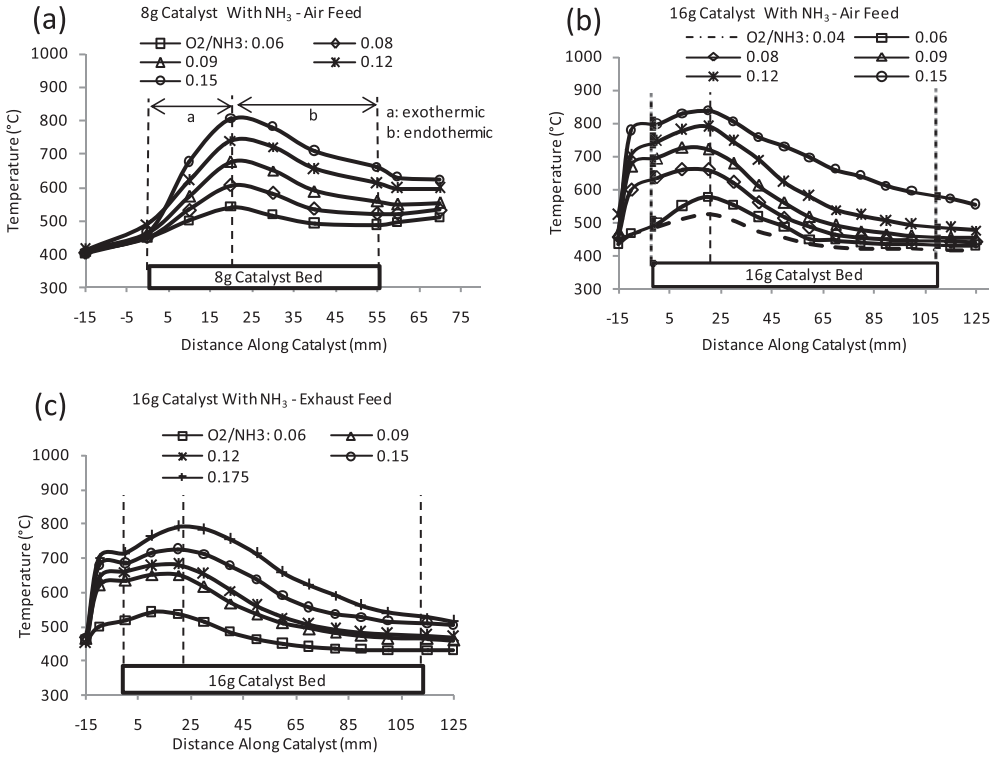

Fig. 3 – Temperature profiles: (a) and (b) temperature profiles of NH_3 - ATR over 8 g and 16 g catalyst beds (c) temperature profiles of NH_3 exhaust gas reforming over 16 g catalyst bed.

amounts (in percentage) of NH_3 decomposed and oxidised are shown separately. The overall NH_3 conversion is presented as the sum of oxidised and decomposed NH_3 excluding any NH_3 slippage. As being consistent to the reaction's thermal behaviour indicated in Fig. 3(a) and (b), the increased O_2/NH_3 ratio enhanced simultaneously the NH_3 oxidation and decomposition. Nevertheless, increasing O_2/NH_3 ratio to 0.175 did not further promote the NH_3 decomposition. However, it suppressed the NH_3 slippage through oxidation: the amount of NH_3 consumed in oxidation reached the maximum. It is also worth noticing that the O_2 content in each individual run was used completely, and no NO, NO_2 or N_2O formation was detected.

In addition to the NH_3 conversion, Fig. 4(b) – (d) plot the produced H_2 as a function of O_2/NH_3 ratio and the NH_3 inlet concentration (at each O_2/NH_3 ratio, see Table 4) for both of the NH_3 – ATR and NH_3 exhaust gas reforming. With more NH_3 decomposed at higher O_2/NH_3 ratios, higher H_2 production was achieved.

Furthermore, the NH_3 inlet concentration at every O_2/NH_3 ratio is identical for NH_3 – ATR over the 8 g and 16 g catalyst beds (the same projected area in Fig. 4 (b) and (c)). Therefore, the improved H_2 production at the 16 g bed confirmed the more favourable reaction conditions provided by the longer catalyst, and is in agreement with the temperature profiles discussed earlier.

Compared to the NH_3 – ATR at the 16 g catalyst, the NH_3 exhaust gas reforming over the same catalyst (Fig. 4(d)) was performed at lower inlet NH_3 concentration at each tested O_2/NH_3 ratio (due to the increased overall inlet flow, Table 4). Although the reactor temperature was reduced during the NH_3 exhaust gas reforming (Fig. 3(c)), at the same O_2/NH_3 ratio, hydrogen production is found to be approximately equivalent to that of the NH_3 – ATR. This observation can be explained by the NH_3 concentration effect shown in Fig. 2(c): less concentrated NH_3 in the exhaust allows ammonia decomposition to perform similarly to that of the NH_3 – ATR, but at lower temperatures.

The hydrogen efficiency (Eq. (4)) and reforming process efficiency (Eq. (5)) of the NH_3 exhaust gas reforming are shown in Fig. 5. Although the hydrogen efficiency was improved at high O_2/NH_3 ratios i.e. higher H_2 production, the reforming process efficiency decreased due to larger NH_3 consumption in exothermic oxidation. Thus a trade – off is shown between these efficiencies. It is suggested that applying the carbon – free reformate (as fuel) to an engine under a low O_2/NH_3 ratio (e.g. 0.06) is expected to be more beneficial in terms of diesel fuel replacement and the engine CO_2 emission.

3.3. *Application of NH_3 exhaust gas reforming in diesel combustion and emission*

In order to study how reformate produced under different efficiencies could affect engine combustion and emissions, the reformate was added into the engine's intake and

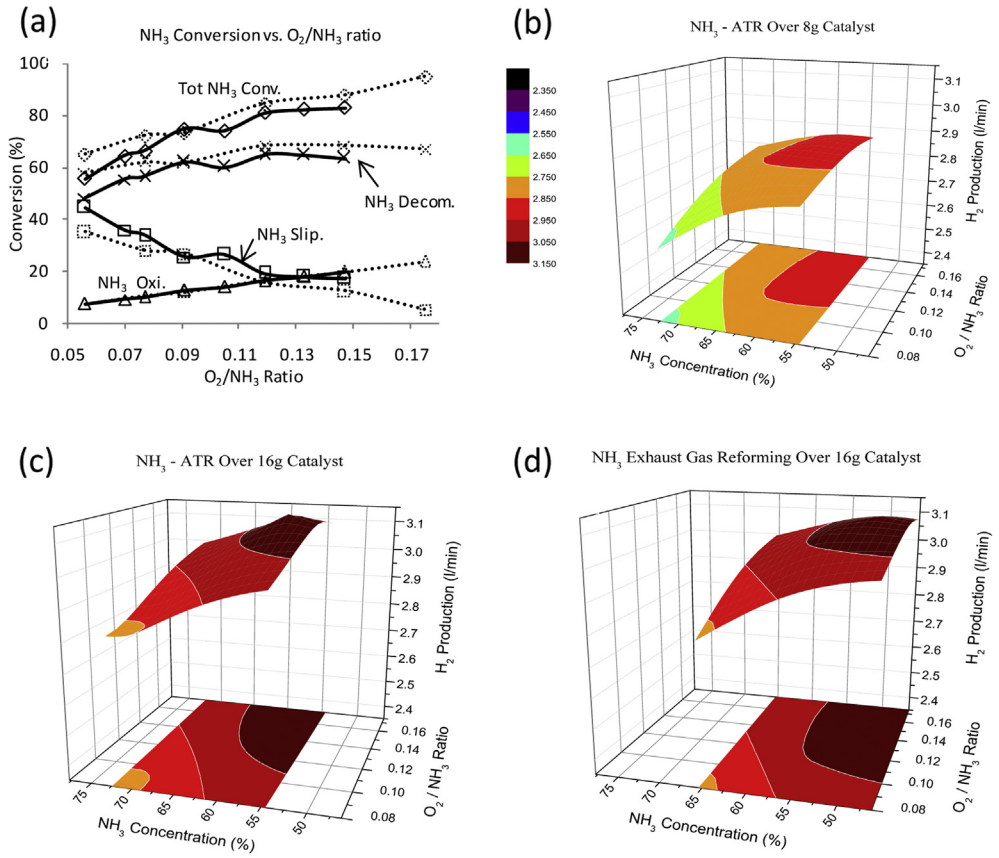

Fig. 4 – (a) NH_3 conversion in NH_3 – ATR at different O_2/NH_3 ratios over 8 g and 16 g catalysts; dotted line: 16 g catalyst, solid line: 8 g catalyst. (b) – (d): H_2 production as a function of NH_3 concentration and O_2/NH_3 ratio; (b) NH_3 – ATR over 8 g catalyst, (c) NH_3 –ATR over 16 g catalyst and (d) NH_3 exhaust gas reforming over 16 g catalyst.

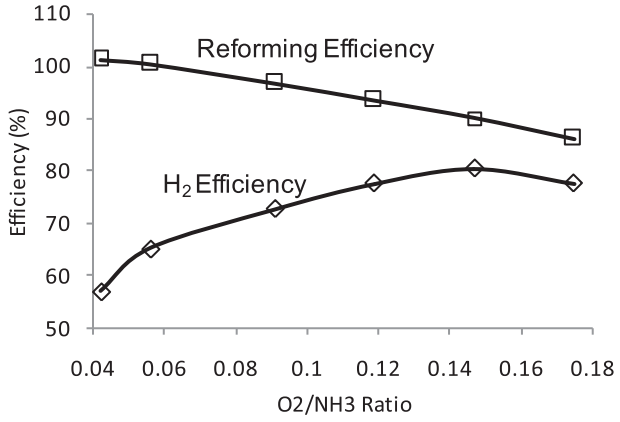

Fig. 5 – Process efficiencies.

combusted as an addition to diesel fuel. Several O_2/NH_3 conditions were selected representing different combinations of H_2 – NH_3 compositions and the reformer efficiencies. The concentrations of the main components, H_2 and unreacted NH_3, were monitored by taking samples of the mixed intake charge. Table 6 lists the engine intake volumetric flow rates of hydrogen and ammonia and their concentrations.

The combustion characteristics are expressed by in-cylinder pressure and rate of heat release (ROHR) in Fig. 6. Compared to the standard diesel operation, the addition of small amount of reformate did not change the combustion pattern significantly. This implies no change in the engine strategy is needed to optimise the combustion.

The brake thermal efficiency (BTE) of the engine at different H_2–NH_3 additions was calculated using Eq. (6)

$$\eta = \frac{P_{Brake}}{(LCV_{diesel} \times \dot{m}_{diesel}) + (LCV_{H_2} \times \dot{m}_{H_2}) + (LCV_{NH_3} \times \dot{m}_{NH_3})} \quad (6)$$

where P_{Brake} is the engine brake power, $\dot{m}$ is the mass flow rate and LCV is the calorific value of each fuel. The BTEs at different reformer-engine fuelling modes are shown in Fig. 7(a).

The addition of the reformate causes a reduction in brake thermal efficiency, but as the H_2 concentration is increased the efficiency reduction decreases. However, Fig. 7(b) shows the use of reformate did result in a 4–5% reduction in injected diesel fuel (to maintain the engine speed and load). These observations indicate the reformate H_2 worked as the primary substituent to the diesel fuel, while the NH_3 was not combusted efficiently, as a result of its high auto – ignition resistance i.e. 651 °C. As shown by Fig. 7(c), with increased reformer – out NH_3 slipping into the intake, the ammonia conversion during the combustion becomes less sufficient, which contributed primarily to the decreased brake thermal efficiency.

As for the engine emissions, replacing the primary diesel by non – carbon based reformate was able to reduce the engine – out carbon emissions. These are reflected by the decreased CO_2, CO and THC shown in Fig. 7(d) – (f). However, with increased NH_3 involved in the combustion, the NH_3 concentration in the exhaust significantly increased, which was ranged from 90 ppm to almost 700 ppm. Apart from its poor combustion, the ammonia emission can also be related to NH_3 being trapped in the combustion chamber crevices and when flame quenching on the chamber walls, i.e. the same mechanisms that are responsible for unburned hydrocarbons in Internal Combustion (IC) engines [16].

Fig. 8 shows the reformate addition increases the NOx emission, which is found in relation to the increased NH_3 at the engine intake. As NH_3 is nitrogen bounded, its oxidation in the combustion process allowed the formation of nitrogen oxides. Therefore, it reveals that the reformer out NH_3 level needs to be controlled to maintain the NOx emission.

As well as the heightened overall NOx emission, the NO_2/NO ratio is substantially increased compared to the pure diesel operation. Based on literature [38,39], this is thought to be caused by the well – known H_2 effect. At low temperatures, peroxy radicals (HO_2 and RO_2) formed during combustion are crucial in promoting NO conversion into NO_2. At relatively cooler in-cylinder temperatures associated with low/medium engine load conditions, a small portion of H_2 – remains uncombusted [40], which can be then mixed with NO – rich combustion products and converted into HO_2, which then reinforces the conversion of NO to NO_2 [38]:

$$HO_2 + NO = NO_2 + OH \quad (7)$$

$$RO_2 + NO = RO + NO_2 \quad (8)$$

The increased NO_2 fraction in the engine exhaust is potentially beneficial as it can be utilised in catalytic aftertreatment systems for NOx and PM removal [41].

Conversely to the energetic benefits postulated earlier with the use of low oxygen to ammonia ratio in the reformer (Fig. 5), the observed engine combustion and emission suggest a use of high purity reformate hydrogen (reformer operated at high O_2/NH_3 ratio), as it is able to replace effectively the carbon fuels, minimise the emitted NH_3 without affecting the engine performance. Although this will incur a reduction in the reforming process efficiency through higher NH_3 oxidation, the amount of NH_3 oxidised at the optimised O_2/NH_3 condition (0.15 in the current study, representing the reforming process that consumed the highest quantity of NH_3 in the oxidative

Table 6 – Reformate flow rates under different reactor conditions and their compositions in the engine intake.

O_2/NH_3	η_{ref} (%)	η_{H_2} (%)	H_2 (engine intake)	NH_3 (engine intake)	Total reformate flow
0.06	102	67	2.6 l/min (5200 ppm)	1.05 l/min (2100 ppm)	3.65 l/min
0.12	95	78	2.9 l/min (5800 ppm)	0.47 l/min (940 ppm)	3.37 l/min
0.15	91	80	3.2 l/min (6340 ppm)	0.29 l/min (580 ppm)	3.49 l/min
0.175	88	77	3.0 l/min (6000 ppm)	0.28 l/min (580 ppm)	3.28 l/min

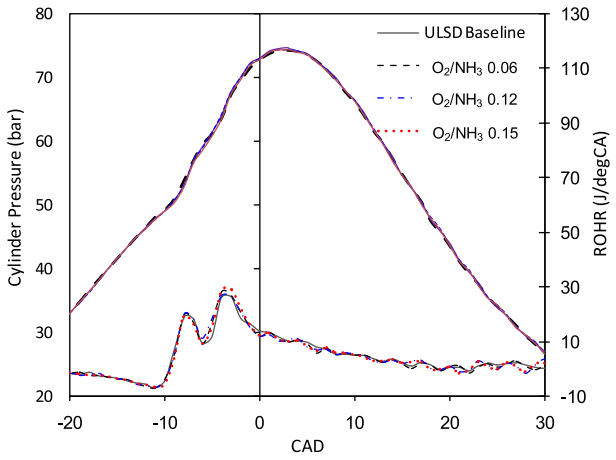

Fig. 6 – Engine in-cylinder pressure and rate of heat release at different reformate additions.

portion) is calculated, using Eq. (9), to present only 1.3% of the total diesel fuel input at the studied engine condition, which indicates a reasonably small fuel penalty.

$$\text{Fuel penalty} = \frac{\dot{m}_{NH_3}(\text{oxidised}) \times \text{LHV}_{NH_3}}{\dot{m}_{ULSD}(\text{input}) \times \text{LHV}_{ULSD}} \times 100\% \quad (9)$$

Where $\dot{m}$ and LCV are the flow rate and calorific value of ULSD and ammonia respectively.

However, to continue using the studied catalyst it is necessary to improve the reactor geometry to reduce the heat loss and strengthen the average reactor temperature. The loss of heat generated both during and following the reaction can be used to improve the overall process efficiency. Recently, Kim et al. [42] provided a detailed study of a microreforming system, where a Micro – Combustor (for NH_3 combustion) and a Micro – Reactor (for NH_3 decomposition) are integrated in cylindrical/annular design for H_2 production. The system's configuration is shown to be effective in heat – recirculation:

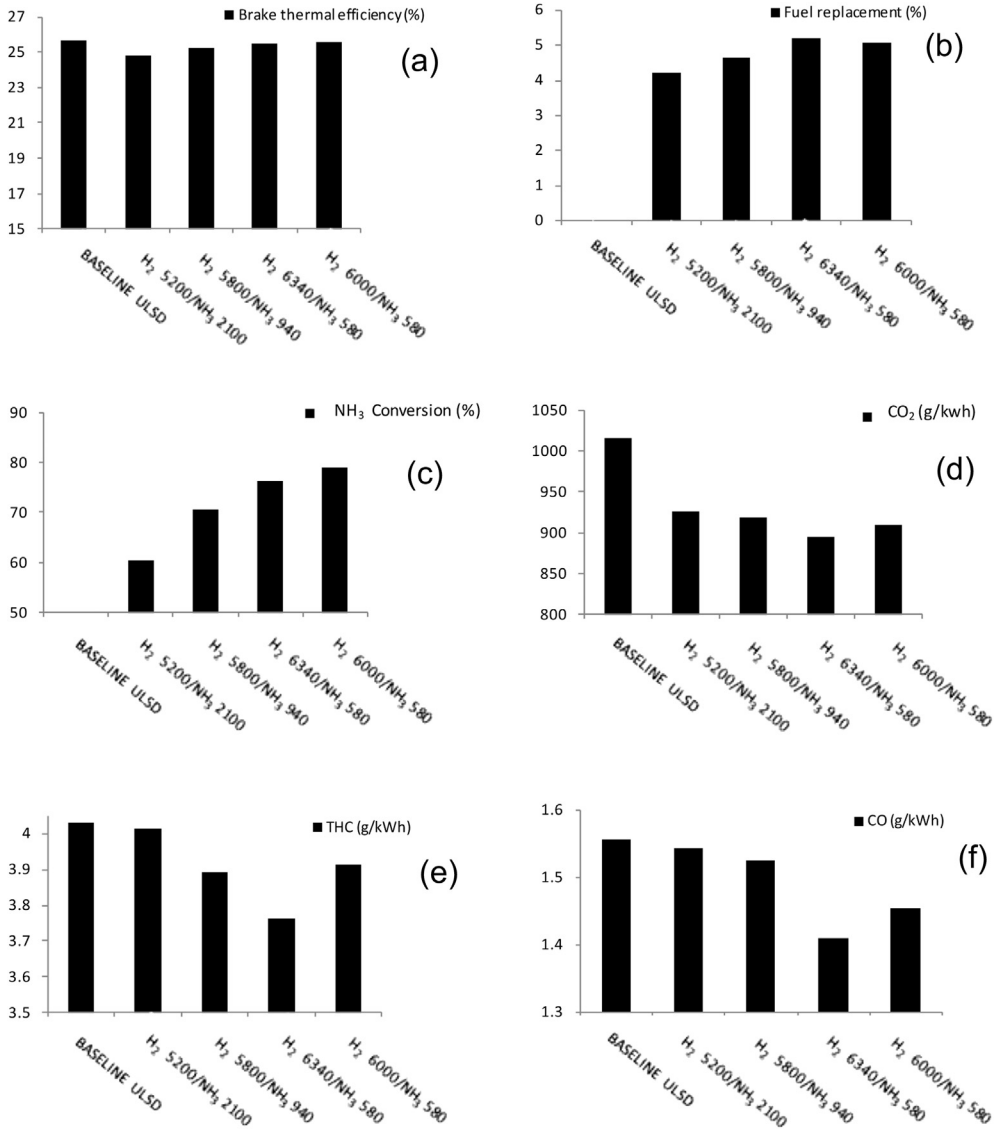

Fig. 7 – (a) engine brake thermal efficiency, (b) diesel fuel replacement, (c) NH_3 conversion during combustion, (d) CO_2 emissions, (e) total hydrocarbon emission, (f) CO emissions.

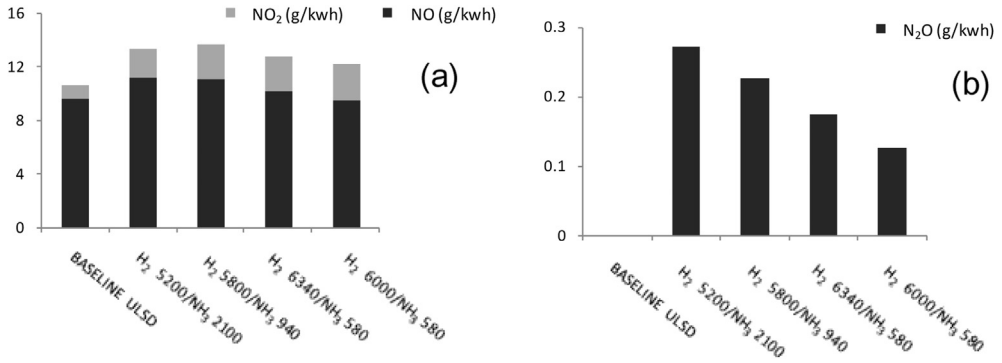

Fig. 8 – Engine NOx emissions: (a) NO_2 and NO emissions, (b) N_2O emission.

extracting heat from exhaust (reacted) gas for preheating fresh reactive mixtures. Hence a similar design can be adopted in the current reformer for better thermal management, leading to improved heat insulation and energy recovery. This would potentially increase the overall process efficiency and further suppress the fuel penalty.

4. Conclusions

From the study presented here, catalytic NH_3 – ATR and ammonia exhaust gas reforming were investigated and proved feasible to produce H_2 on board. The O_2/NH_3 ratio and its corresponding NH_3 concentration in the gas feed as well as the GHSV were found to impact the H_2 yield. A combination of these factors leads to different NH_3 conversion, gas product composition and reaction efficiencies.

When the carbon – free reformate was introduced into the engine intake, part of the primary diesel was replaced and the engine's carbon emissions (CO_2, CO and THC) were reduced. The engine out NO_2/NO ratio increased substantially, which is potentially beneficial to diesel aftertreatment system (DPF passive regeneration, SCR DeNOx activity at low temperature and etc.). However, excessive NH_3 addition resulted in inefficient use of the reforming products, deteriorated engine out NOx emission level and undesired NH_3 slippage in the exhaust. Hence, without engine modification/optimisation, the direct use of NH_3 (as fuel) in diesel combustion could be regarded as inappropriate. Ammonia's potential in delivering hydrogen should be magnified by adopting the studied reformer system, at conditions that produce high purity of H_2. Nevertheless, the presence of NH_3 in the exhaust could be beneficial to certain aftertreatment devices (NH_3 – SCR), which will utilise the emitted NH_3 in further reactions to control the overall engine emission.

Acknowledgements

The authors would like to thank Johnson Matthey for funding the project and providing the catalysts. The School of Mechanical Engineering at the University of Birmingham (UK) is gratefully acknowledged for the PhD School Scholarship to Mr. Wentao Wang. Engineering and Physical Science Research Council – EPSRC projects (EP/G038139/1) and the Advantage West Midlands and the European Regional Development Fund as part of the Science City Research Alliance Energy Efficiency Project are also acknowledged for supporting the research work.

REFERENCES

[1] Golunski S. What is the point of on-board fuel reforming? Energy Environ Sci 2010;3:1918–23.
[2] Abu-Jrai A, Tsolakis A, Megaritis A. The influence of and CO on diesel engine combustion characteristics, exhaust gas emissions, and after treatment selective catalytic reduction. Int J Hydrogen Energy 2007;32:3565–71.
[3] Rodríguez-Fernández J, Tsolakis A, Cracknell RF, Clark RH. Combining GTL fuel, reformed EGR and HC-SCR after treatment system to reduce diesel NOx emissions. A statistical approach. Int J Hydrogen Energy 2009;34:2789–99.
[4] Abu-Jrai A, Tsolakis A. The effect of H and CO on the selective catalytic reduction of NO under real diesel engine exhaust conditions over Pt/AlO. Int J Hydrogen Energy 2007;32:2073–80.
[5] Plana C, Armenise S, Monzón A, García-Bordejé E. Ni on alumina-coated cordierite monoliths for in situ generation of CO-free H_2 from ammonia. J Catal 2010;275:228–35.
[6] Martin S, Wörner A. On-board reforming of biodiesel and bioethanol for high temperature PEM fuel cells: comparison of autothermal reforming and steam reforming. J Power Sources 2011;196:3163–71.
[7] Wu C, Williams PT. A novel nano-Ni/SiO_2 catalyst for hydrogen production from steam reforming of ethanol. Environ Sci Technol 2010;44:5993–8.
[8] Tsolakis A, Megaritis A, Golunski SE. Reaction profiles during exhaust-assisted reforming of diesel engine fuels. Energy & Fuels 2005;19:744–52.
[9] Chen J, Zhu ZH, Wang S, Ma Q, Rudolph V, Lu GQ. Effects of nitrogen doping on the structure of carbon nanotubes (CNTs) and activity of Ru/CNTs in ammonia decomposition. Chem Eng J 2010;156:404–10.
[10] Wang SJ, Yin SF, Li L, Xu BQ, Ng CF, Au CT. Investigation on modification of Ru/CNTs catalyst for the generation of COx-free hydrogen from ammonia. Appl Catal B 2004;52:287–99.
[11] Zhang J, Xu H, Li W. Kinetic study of NH3 decomposition over Ni nanoparticles: the role of La promoter, structure

sensitivity and compensation effect. Appl Catal A 2005;296:257–67.
[12] Chellappa AS, Fischer CM, Thomson WJ. Ammonia decomposition kinetics over Ni–Pt/Al_2O_3 for PEM fuel cell applications. Appl Catal A 2002;227:231–40.
[13] Zamfirescu C, Dincer I. Ammonia as a green fuel and hydrogen source for vehicular applications. Fuel Process Technol 2009;90:729–37.
[14] Klerke A, Christensen CH, Norskov JK, Vegge T. Ammonia for hydrogen storage: challenges and opportunities. J Mater Chem 2008;18:2304–10.
[15] Kim JH, Kwon OC. A micro reforming system integrated with a heat-recirculating micro-combustor to produce hydrogen from ammonia. Int J Hydrogen Energy 2011;36:1974–83.
[16] Reiter AJ, Kong S-C. Combustion and emissions characteristics of compression-ignition engine using dual ammonia-diesel fuel. Fuel 2011;90:87–97.
[17] Gill SS, Chatha GS, Tsolakis A, Golunski SE, York APE. Assessing the effects of partially decarbonising a diesel engine by co-fuelling with dissociated ammonia. Int J Hydrogen Energy 2012;37:6074–83.
[18] Schlapbach L, Zuttel A. Hydrogen-storage materials for mobile applications. Nature 2001;114:353–8.
[19] Christensen CH, Johannessen T, Sørensen RZ, Nørskov JK. Towards an ammonia-mediated hydrogen economy? Catal Today 2006;111:140–4.
[20] Zamfirescu C, Dincer I. Using ammonia as a sustainable fuel. J Power Sources 2008;185:459–65.
[21] Zamfirescu C, Dincer I. Utilization of hydrogen produced from urea on board to improve performance of vehicles. Int J Hydrogen Energy 2011;36:11425–32.
[22] Yin S-F, Zhang Q-H, Xu B-Q, Zhu W-X, Ng C-F, Au C-T. Investigation on the catalysis of COx-free hydrogen generation from ammonia. J Catal 2004;224:384–96.
[23] Ganley JC, Seebauer EG, Masel RI. Development of a microreactor for the production of hydrogen from ammonia. J Power Sources 2004;137:53–61.
[24] Yosuke S, Hiroshi M, Tetsuo N, Yuji A, Takashi S. Hydrogen generation system with ammonia cracking for a fuel-cell electric vehicle. SAE Tech Paper 2009. 2009-01-1901.
[25] Schriber TJ, Parravano G. The low temperature oxidation of ammonia over a supported ruthenium catalyst. Chem Eng Sci 1967;22:1067–78.
[26] Ng PF, Li L, Wang S, Zhu Z, Lu G, Yan Z. Catalytic ammonia decomposition over industrial-waste-supported Ru catalysts. Environ Sci Technol 2007;41:3758–62.
[27] Gay SE, Ehsani M. Ammonia hydrogen carrier for fuel cell based transportation. SAE Technical Paper 2003. 2003-01-2251.
[28] Ishimatsu S, Saika T, Nohara T. Ammonia fueled fuel cell Vehicle:The new concept of a hydrogen supply system. SAE Technical Paper 2004. 2004-01-1925.
[29] Chein R-Y, Chen Y-C, Chang C-S, Chung JN. Numerical modeling of hydrogen production from ammonia decomposition for fuel cell applications. Int J Hydrogen Energy 2010;35:589–97.
[30] Prasad V, Karim AM, Arya A, Vlachos DG. Assessment of overall rate expressions and multiscale, microkinetic model uniqueness via experimental data injection: ammonia decomposition on Ru/γ-Al_2O_3 for hydrogen production. Ind Eng Chem Res 2009;48:5255–65.
[31] Tsai W, Vajo JJ, Weinberg WH. Inhibition by hydrogen of the heterogeneous decomposition of ammonia on platinum. J Phys Chem 1985;89:4926–32.
[32] Zheng W, Zhang J, Xu H, Li W. Decomposition kinetics on supported Ru clusters: morphology and particle size effect. Catal Lett 2007;119:311–8.
[33] Bradford MCJ, Fanning PE, Vannice MA. Kinetics of NH_3 decomposition over well dispersed Ru. J Catal 1997;172:479–84.
[34] Löffler DG, Schmidt LD. Kinetics of NH_3 decomposition on iron at high temperatures. J Catal 1976;44:244–58.
[35] Lau CS, Tsolakis A, Wyszynski ML. Biogas upgrade to syn-gas (H_2–CO) via dry and oxidative reforming. Int J Hydrogen Energy 2011;36:397–404.
[36] Tsolakis A, Golunski SE. Sensitivity of process efficiency to reaction routes in exhaust-gas reforming of diesel fuel. Chem Eng J 2006;117:131–6.
[37] Ladommatos N, Abdelhalim S, Zhao H. The effects of exhuast gas recirculation on diesel combustion and emissions. Int J Engine 2000;1:107–26.
[38] Varde KS, Frame GA. Hydrogen aspiration in a direct injection type diesel engine-its effects on smoke and other engine performance parameters. Int J Hydrogen Energy 1983;8:549–55.
[39] Lilik GK, Zhang H, Herreros JM, Haworth DC, Boehman AL. Hydrogen assisted diesel combustion. Int J Hydrogen Energy 2010;35:4382–98.
[40] Liu S, Li H, Liew C, Gatts T, Wayne S, Shade B, et al. An experimental investigation of NO_2 emission characteristics of a heavy-duty H_2-diesel dual fuel engine. Int J Hydrogen Energy 2011;36:12015–24.
[41] Gill SS, Chatha GS, Tsolakis A. Analysis of reformed EGR on the performance of a diesel particulate filter. Int J Hydrogen Energy 2011;36:10089–99.
[42] Kim JH, Um DH, Kwon OC. Hydrogen production from burning and reforming of ammonia in a microreforming system. Energy Conversion Manage 2012;56:184–91.